

Character and stability of a wind-driven supercooled water film on an icing surface—II. Transition and turbulent heat transfer

A.R. Karev^a, M. Farzaneh^{a,*}, E.P. Lozowski^b

^a NSERC/Hydro-Québec/UQAC Industrial Chair on Atmospheric Icing of Power Network Equipment (CIGELE), Université du Québec à Chicoutimi, 555 Boulevard de l'Université, Chicoutimi, PQ, Canada G7H 2B1

^b Department of Earth and Atmospheric Sciences, University of Alberta, Edmonton, AB, Canada T6G 2E3

Received 13 February 2002; accepted 18 June 2002

Abstract

In the accompanying paper [A.R. Karev et al., *Internat. J. Therm. Sci.* 42 (2003), this issue] and the present one, the problem of the appearance and disappearance of the thin water film flowing over an accreting ice surface is reformulated as a problem of the flow dynamics of this water film, taking into consideration both laminar and turbulent heat transfer from the ice/water interface. By comparing the different responses of the rate of ice growth in the supercooled flowing water film, to sudden disturbances in the film thickness, for both laminar and turbulent heat transfer regimes, a new explanation is offered for “wet” and “dry” icing regimes. This explanation is an improvement over the existing one [B.L. Messinger, *J. Aero. Sci.* 20 (1953) 29–42], which is based on macroscopic heat balance considerations. Our solution considers a microscopic heat balance analysis, related to the kinetics of crystal growth, and allows for a finite supercooling at the ice/water interface, relative to the fusion temperature of water, T_m . In the present paper, the kinetics of freezing of a supercooled water film flowing over an icing surface are examined in relation to turbulent heat transfer through the water film. The occurrence of turbulence in the supercooled water film is found to be the determining factor contributing to its stability during freezing under fluctuating external thermodynamic conditions.

© 2002 Éditions scientifiques et médicales Elsevier SAS. All rights reserved.

Keywords: Supercooled water film; Ice accretion; Linear rate of crystallization; Turbulent Couette flow

1. Introduction

In the accompanying paper [1], the kinetics of freezing of a supercooled water film, flowing over an accreting ice surface, were considered in relation to laminar heat transfer through the water film. The paper investigated the response of the ice growth rate to short-term fluctuations of one or several thermodynamic parameters, resulting in sudden disturbances in the thickness of the water film. The solution was conditioned by assuming the following facts:

- (i) absence of appreciable heat conduction into the already-formed ice deposit;
- (ii) an isothermal ice/water interface; and
- (iii) quasi-steady external thermodynamic conditions as a consequence of assumed laminar flow in both the air–

aerosol and the water film, with either constant heat flux or constant temperature boundary conditions at the water surface.

It was shown that, given these assumptions, the laminar regime of a shear-driven supercooled water film, with a nearly-linear temperature profile, is unstable. The instability consists of irreversible changes in the water film thickness in the direction of its initial disturbance. If the water film thins initially, there occurs a rapid disappearance of the film. If it thickens initially, the process continues until the liquid film achieves a stable turbulent flow. This behavior was attributed to the absence of a significant longitudinal temperature gradient in the developed laminar flow, and hence, to an inability appreciably to change the convection following disturbances in the thickness of the water film. Convection has a significant influence on the ultimate change in the water film thickness over a very small range of longitudinal distance only, near the origin of the flow, where the temperature field is still developing. Between these two

* Corresponding author.

E-mail address: farzaneh@uqac.quebec.ca (M. Farzaneh).

URL address: <http://icevolt.uqac.quebec.ca/cigele>.

zones, lies an intermediate narrow range of longitudinal distance, where the rate of ice growth exhibits no reaction to changes in the thickness of the water film.

In what follows, it will be shown that, under similar assumptions, the turbulent heat transfer regime is stable for a shear-driven, supercooled water film, flowing over a growing ice surface. Stability here means a restoration of the water film thickness to its initial value, subsequent to a disturbance resulting from a sudden change in any of the thermodynamic parameters. The solution will be conditioned by assuming the following:

- (i) absence of appreciable heat conduction into the already-formed ice deposit;
- (ii) negligible convective heat transfer in comparison with the turbulent heat transfer; and
- (iii) the external heat transfer at the surface of the flowing turbulent water film is a consequence of turbulent flow in both the air–aerosol and the water film.

This stable behaviour is explained by the rapid adjustment of the turbulent heat transfer through the film to sudden disturbances, due to changes in the thermal eddy diffusivity, ε_H , through the disturbed water film thickness. This behaviour is a basis for the offered new explanation for “wet” and “dry” icing regimes as an improvement over the existing one [2].

2. Formulation of the problem and principal assumptions

We begin here with the formulation of the problem, as it has been presented in the accompanying paper [1]. We consider an icing object located within a supercooled air–aerosol flow, and suppose that a thin turbulent water film, flowing under the influence of a constant air shear stress, F , has formed on the icing surface. Suppose that the layer lying immediately adjacent to the surface of the structure has already turned into ice (Fig. 1). A turbulent–turbulent combination of regimes is examined here, for parallel flows

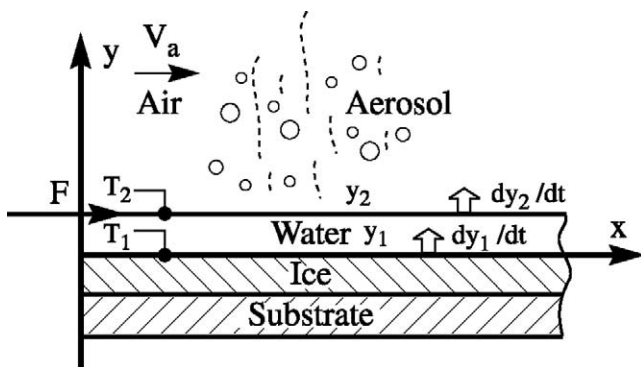


Fig. 1. Schematic of a thin, supercooled water film flowing on the surface of accreted ice in the “wet” regime.

in the air–aerosol and in the water film; that is, the flow in both the air–aerosol and the water film is presumed to be turbulent. As in [1], we will focus on how fluctuations of one or several thermodynamic parameters, causing changes in the thickness of the water film, can influence the rate of ice growth beneath the supercooled flowing water. The equations for turbulent transfer of x -momentum and heat, in the thin water film flowing over the accreting ice surface, may be written as follows:

$$\frac{\partial}{\partial y} \left\{ (v_w + \varepsilon_M) \frac{\partial u}{\partial y} \right\} = 0 \quad (1)$$

$$\frac{\partial}{\partial y} \left\{ (\chi_w + \varepsilon_H) \frac{\partial T}{\partial y} \right\} = \frac{\partial}{\partial y} \left\{ \left(\frac{v_w}{Pr} + \frac{\varepsilon_M}{Pr_t} \right) \frac{\partial T}{\partial y} \right\} = 0 \quad (2)$$

where the following nomenclature is used for the properties of water: ν_w and χ_w are the kinematic viscosity and thermal diffusivity ($\text{m}^2 \cdot \text{s}^{-1}$), respectively; ε_M and ε_H are eddy diffusivities for momentum and heat transfer ($\text{m}^2 \cdot \text{s}^{-1}$), respectively; Pr and Pr_t are the molecular and turbulent Prandtl numbers, respectively; $u(y)$ is the tangential component of velocity ($\text{m} \cdot \text{s}^{-1}$); and $T(x, y)$ is the temperature field in the supercooled water film (K). The normal component of velocity in the boundary layer is considered to be negligible in comparison with the tangential component. In Eq. (2), it is assumed that the turbulent heat transfer is considerably greater than that of the convective heat transfer. Application of a constant shear stress condition at the air–aerosol/water interface and a no-slip condition at the ice/water interface yields two boundary conditions for the x -momentum:

$$\left. \frac{\partial u}{\partial y} \right|_{y=y_2} = \frac{F}{\rho_w \nu_w} \quad (3)$$

$$u|_{y=y_1} = 0 \quad (4)$$

where F is the interfacial shear stress at the surface of the liquid film ($\text{N} \cdot \text{m}^{-2}$); and ρ_w is the water density ($\text{kg} \cdot \text{m}^{-3}$). As in [1], a constant interfacial shear stress will be considered here for the ideal case of a smooth free surface without surface waves, having constant pressure in the liquid film as a consequence. In future research, the real enhanced air shear stress, as produced by natural surface disturbances, could be taken into account by using experimental data. It was shown in [1] that the simple empirical formula proposed by Cheremisinoff and Davis [3], deduced from previous experimental measurements made by Miya et al. (reference in [3]), may be applied very successfully in this case. By rearranging this formula, one obtains:

$$F = \frac{4 \times 10^{-3} \rho_a V_a^2}{1 - 2 \times 10^{-5} \frac{h^2 \rho_a V_a^2}{4 \rho_w \nu_w^2}} \quad (5)$$

where: ρ_a is the air density ($\text{kg} \cdot \text{m}^{-3}$); V_a the air speed ($\text{m} \cdot \text{s}^{-1}$); and h the water film thickness (m). In order to preserve the range of applicability of this formula, the following inequality must be imposed:

$$\frac{F}{200} \geq \frac{\rho_w \nu_w^2}{h^2} \geq \frac{F}{3400} \quad (6)$$

If these limits are exceeded, however, the appropriate limiting value for the interfacial shear stress should be assumed.

The first boundary condition for the heat transfer equation will consist of a modified Stefan problem, taking into account the additional turbulent heat transfer and the presence of a finite supercooling imposed at the ice/water interface:

$$-\rho_w c_w \cdot \left(\chi_w + \frac{\varepsilon_M}{Pr_t} \right) \cdot \frac{\partial T}{\partial y} \Big|_{y=y_1} = \rho_i L_i \frac{dy_1}{dt} \quad (7)$$

where c_w is the specific heat capacity of water ($\text{J}\cdot\text{kg}^{-1}\cdot\text{K}^{-1}$); ρ_i is the density of the growing ice layer at the interface y_1 ($\text{kg}\cdot\text{m}^{-3}$) whose rate of displacement is dy_1/dt ($\text{m}\cdot\text{s}^{-1}$); t is time (s); L_i is the specific latent heat of freezing of water at 0°C ($\text{J}\cdot\text{kg}^{-1}$). As stated in [1], turbulence may be produced by waves at the air/water interface, or by water flow moving past the growing ice crystals at the water/ice interface, y_1 , where the growing crystals are considered as “roughness elements”. Although turbulence is absent in the laminar sub-layer near the ice/water interface, the second term on the left-hand side is retained to account for the case of a “thermally rough” surface, where the heat flux is considered to arise from the tips of the ice crystals which reach into the buffer zone. For the purposes of the present paper, the ice/water interface is considered to be rough.

The second boundary condition for the heat transfer equation accounts for the presence of a finite supercooling, Δ_1 , relative to the fusion temperature, T_m , at the ice/water interface:

$$T|_{y=y_1} = T_1 = T_m - \Delta_1 \quad (8)$$

The equation defining this supercooling, which is the motive power for ice/water interface growth on a microscopic scale [4], may be written as follows:

$$\frac{dy_1}{dt} = a \cdot \Delta_1^b = a \cdot (T_m - T_1)^b \quad (9)$$

where a ($\text{m}\cdot\text{s}^{-1}\cdot\text{K}^{-b}$) and b are empirical constants. The second equation, which completes the mass balance, describes the displacement of the air–aerosol/water interface, normal to the water film flow, resulting from the flux of impinging water droplets:

$$\frac{dy_2}{dt} = \frac{w \cdot \bar{E} \cdot V_a}{\rho_w} - C_e \quad (10)$$

where dy_2/dt is the growth velocity of the water film surface ($\text{m}\cdot\text{s}^{-1}$); w is the liquid water content (LWC) of the air–aerosol flow ($\text{kg}\cdot\text{m}^{-3}$); \bar{E} is the mean transfer efficiency of the dispersed phase, from the aerosol onto the surface of the water film (i.e., the entrainment or collection efficiency [1]); and C_e is a correction to the rate of displacement of the air/water surface arising from evaporation ($\text{m}\cdot\text{s}^{-1}$). Unlike the order of magnitude of the inflow and discharge of water, dy_1/dt and dy_2/dt are of similar orders of magnitude. In order to determine the stability of the system, its equilibrium must first be determined, when the rates of displacement

of both surfaces are equal. Then, the reaction of dy_1/dt to sudden changes in dy_2/dt , which leads to corresponding changes in the water film thickness, must be investigated.

3. Turbulence modeling of momentum and heat transfer

The onset of the transition to turbulent water film flow on an icing surface will be investigated elsewhere. Here, it is taken as a given that the turbulent state has already been attained. The solutions to Eqs. (1) and (2), based on this fact, may be obtained either with one- or two-equation turbulence modeling, or with algebraic modeling of the eddy diffusivity for momentum transfer.

3.1. Velocity profile of a turbulent water film under a wavy water/air interface

By using the following definitions

$$u_\tau = \sqrt{\tau_{wl}/\rho_w} \quad (11)$$

$$y^+ = u_\tau \cdot y/\nu_w \quad (12)$$

$$u^+ = u/u_\tau \quad (13)$$

(1) may be transformed into the non-dimensional equation:

$$\frac{\partial}{\partial y^+} \left\{ \left(1 + \frac{\varepsilon_M}{\nu_w} \right) \frac{\partial u^+}{\partial y^+} \right\} = \frac{\partial}{\partial y^+} \left\{ (1 + \varepsilon_M^+) \frac{\partial u^+}{\partial y^+} \right\} = 0 \quad (14)$$

where τ_{wl} is the wall shear stress ($\text{N}\cdot\text{m}^{-2}$); u_τ is the wall skin velocity ($\text{m}\cdot\text{s}^{-1}$), and y^+ and u^+ are the dimensionless coordinates in the direction normal to the main flow, and the dimensionless velocity of the water film flow, respectively. The dimensionless eddy diffusivity is defined by: $\varepsilon_M^+ = \varepsilon_M/\nu_w$.

Eq. (14) is the usual dimensionless formulation for turbulent Couette flow. From the classical formulation for the total dimensionless shear stress, τ^+ , it follows that:

$$\begin{aligned} \tau^+ &= \frac{\tau}{\tau_{wl}} = \frac{\tau_t + \tau_{vis}}{\tau_{wl}} = \frac{\varepsilon_M}{\nu_w} \cdot \frac{du^+}{dy^+} + \frac{du^+}{dy^+} \\ &= (1 + \varepsilon_M^+) \cdot \frac{du^+}{dy^+} \end{aligned} \quad (15)$$

where, τ is the total shear stress in the water film ($\text{N}\cdot\text{m}^{-2}$), which is the sum of the laminar shear stress, τ_{vis} , and an additional turbulent shear stress, τ_t , itself resulting from eddy momentum transfer; and τ^+ is the dimensionless equivalent of the total shear stress. By comparing (14) and (15), we infer that the total shear stress remains constant through the entire water film thickness. In the last term on the right-hand side of Eq. (15), it was assumed that the turbulent shear stress vanishes at the wall, and as a result that $\tau_{vis} = \tau_{wl}$. If the turbulence also vanishes near the air–aerosol/water interface (to be discussed in the next section), then an equality of the wall and interfacial shear stresses

$\tau_{wl} = F$ follows automatically. In such a case, the equation for the water film velocity profile may be written as:

$$u^+ = \int_0^{y^+} \frac{1}{1 + \varepsilon_m^+} dy^+ \quad (16)$$

From these last equations, it may be concluded, that determining the eddy diffusivity for momentum transfer, through the entire film thickness, is a key factor for algebraic modeling of the turbulent liquid film. Once the velocity profile has been determined, the Reynolds number of the water film, defined through the mass flow rate, may be calculated as follows:

$$Re_{FL} = 4 \frac{\Gamma}{\mu_w} = 4 \int_0^{h^+} u^+ dy^+ \quad (17)$$

where Γ is mass flow rate per unit of film width ($\text{kg} \cdot \text{m}^{-1} \cdot \text{s}^{-1}$), while $h^+ = u_\tau \cdot h / \nu_w$ is the dimensionless water film thickness, defined by analogy with the definition of scale in the distance normal to the flow, i.e., Eq. (12). In the following section, two appropriate algebraic models of eddy diffusivity for momentum transfer will be proposed, and the rationale for such a choice will be provided.

3.2. Turbulence structure and relevant algebraic model

The turbulence field in thin, shear-driven water films presents several levels of complexity due to having a combined source in both the wave-sheared air–water interface and the shear near the wall. Moreover, due to the thinness of the films, their turbulence structure has, so far, been poorly investigated. Nevertheless, many empirical and semi-empirical models exist, particularly, for freely-falling turbulent liquid films [5]. In contrast, the corresponding turbulence structure in channel flows has been carefully studied. Recently, Komori et al. [6] found that the structure of turbulent mass transfer across the sheared air/water interface in channels is very similar to that in thin films. Although in the latest experimental investigations [7], the minute eddies characterizing organized motion at the wavy surface were not found in a thin liquid layer, ($O \sim \text{mm}$), compared with a deep liquid layer, ($O \sim m$), the general turbulence structure in both cases was found to be similar to a large degree. This leads us to suppose that turbulent transfer mechanisms, i.e., heat and momentum transfers, in both cases, are nearly identical as well. Thus, the experimental data from channel flow will be applied to thin liquid films. Similar considerations have been made for freely-falling films [5].

The structures of the turbulence field in an open channel flow, involving a free water surface, and a sheared wavy water surface, are distinct from one another. Although the velocity field near the wall, in both of the above cases, can be represented by van Driest's eddy diffusivity model [8], this field is completely different in the region of the water/air

interface. Van Driest's eddy diffusivity model, with the damping layer merging into a logarithmic law in the fully turbulent region, may be written as follows:

$$\varepsilon_M^+ = \frac{\varepsilon_M}{\nu_w} = -0.5 + 0.5 \sqrt{1 + 4K^2 y^{+2} [1 - \exp(-y^+/A^+)]^2} \quad (18)$$

where K is von Karman's constant, $K = 0.4$; and A^+ is van Driest's empirical damping constant, $A^+ = 26$.

In a channel flow with a free water surface, fluctuations of the normal velocity in the water cease near the free surface, due to the combined effects of surface tension and gravity [9]. This constraint gives rise to increased streamwise and lateral motions in this region, however, promoting increased turbulent velocity fluctuations in each of the directions mentioned. Temperature fluctuations, on the other hand, are greatest near the free surface. Levich [10], on the basis of theoretical suppositions, assumed that surface tension could be a stabilizing factor, eliminating normal turbulent velocity fluctuations near the free surface. He called the layer over which the surface tension influence extends a "diffusion sublayer". According to Levich, its thickness, h_σ , may be defined as follows, using dimensional considerations:

$$h_\sigma = \left(\frac{\sigma_{w-a} \cdot \nu_w}{\rho_w \cdot \hat{v}'^3} \right)^{1/2} \quad (19)$$

where σ_{w-a} is the surface tension at the boundary between the water and air ($\text{kg} \cdot \text{s}^{-2}$); and \hat{v}' is the root-mean-square (rms) fluctuation of the normal velocity component in water ($\text{m} \cdot \text{s}^{-1}$).

Powerful bursts from the wall region, i.e., the solid/liquid interface, are considered to be the source of the turbulence. Levich [10] also proposed that the eddy diffusivity near the solid/fluid interface should vary as the third power of normal distance from the wall. This is allowed for in van Driest's model (18). In the vicinity of the fluid/fluid interface, however, according to Levich [10], eddy diffusivity varies as the second power of normal distance from the wall. In summary, for the case of a free liquid surface, the eddy diffusivity in the direction normal to the main flow, should increase from zero near the wall, as the third power of the normal distance from the wall, then reach a maximum in the bulk flow, and finally, at a depth defined by Eq. (19), begin to decrease to zero once again at the free surface, as the second power of the normal distance from the wall. The algebraic eddy diffusivity model for turbulent water flow in a channel with a free surface, based on slightly different considerations [11], has a similar overall eddy diffusivity distribution in the liquid. An asymmetry in its distribution over the liquid layer, especially for larger wavelengths, may be noted as well. Application of the logarithmic profile to the bulk of the water flow led Ueda et al. [11] to the following equation that does not include damping:

$$\varepsilon_M^+ = K y^+ \left(1 - \frac{y^+}{h^+} \right) \quad (20)$$

In the case of a rough solid/liquid interface, the rise near the wall should be steeper without a damping layer [8]. Such a one-dimensional turbulence model could be applied to the case of gravitational flow of a water film over an icing surface, e.g., for the mechanism of icicle formation under conditions of free or mixed convection. A two-dimensional eddy-diffusivity model analogous to that presented in [12] (i.e., a model with two eddy diffusivities in the two coordinate directions), must consider a secondary maximum for the streamwise component of eddy diffusivity near the free surface, owing to the redistribution of turbulent kinetic energy, as mentioned earlier.

In the case of a turbulent, shear-driven liquid in a channel, the presence of waves on its surface is a supplementary source of turbulence. This additional turbulent energy is thought to be produced by the microbursts upstream of the crests [13]. Consequently, the total turbulence intensity in the liquid layer, with a concurrent wavy gas-liquid flow, has an approximately constant value over the bulk of the flow, increasing slightly near the free surface, and increasing relatively more in the near-the-wall region. The complex interaction of two turbulence fields, created near the wall and near the wavy surface, results in the formation of a vortex structure [14]. Consequently, it would appear that the classical modified surface renewal eddy diffusivity model [9], with a pre-defined frequency of surface renewal motions on the water side of the water/air interface, f_{wr} , is not appropriate here. The frequency, f_{wr} , can presumably be related to the amplitude, wavelength, and frequency of the waves. To the best of our knowledge, however, a complete theory of this kind has not yet been formulated.

The mass transfer intensity in any surface renewal model is generally known to be proportional to the square root of the frequency of surface renewal motion, $f_{wr}^{1/2}$. Komori et al. [6] found experimentally, that a strong relationship exists between $f_{wr}^{1/2}$ and the friction velocity, u_{a-w} , at the wavy air/water interface. In the high shear region, the rate of increase of $f_{wr}^{1/2}$ diminishes with increasing values of u_{a-w} , tending towards saturation. This suggests a saturation of the turbulent transfer mechanism near the wavy water/air interface, for high shears ($u_{a-w} \geq 0.25 \text{ m}\cdot\text{s}^{-1}$). These observations indicate the importance and advantages of using an interfacial shear stress approach in the eddy diffusivity model, instead of a surface renewal model, for the region $u_{a-w} \leq 0.25 \text{ m}\cdot\text{s}^{-1}$. In order to investigate the effect of interfacial shear stress on the momentum and heat transfer, the model developed by Hubbard et al. [15] will be applied in our next investigation. Their model consists of two equations for eddy diffusivity near the wall and near the liquid-air interface, respectively, overlapping at their point of intersection. The second equation, which is an empirical description of the results of experimental measurements of adsorption in the surface layer of thin films, proposes a variation of eddy diffusivity with the second power of the normal distance from the wall, exactly as proposed by Levich [10]. In the present investigation, for

ease of calculation, we also consider Mudawwar and El-Masri's model [5] for heat transfer across a freely falling, turbulent water film, heated from below. The results obtained with models for heat transfer through a turbulent water film heated from below will be compared to the results obtained with a near-the-wall eddy diffusivity model [8]. Both models mentioned for use with a turbulent water film were developed for its gravitational flow only, including the dependence of the heat transfer on the Reynolds number, Re_{FL} , the Prandtl number, Pr , and the Kapitza number, Ka , especially in the region $Re_{FL} < 10^4$. A few words should be said about the adjustment of the models to the case of a shear-driven film. The newly introduced dimensionless Kapitza number, Ka , is defined by:

$$Ka = \frac{\mu_w^4 g}{\rho_w \sigma_{w-a}^3} \quad (21)$$

where μ_w is the dynamic viscosity of water ($\text{kg}\cdot\text{m}^{-1}\cdot\text{s}^{-1}$); and g is the acceleration due to gravity ($\text{m}\cdot\text{s}^{-2}$). It may be said that Ka explains the extension of the damping layer near the air/water interface, due to surface tension, as defined by Eq. (19). Ka can also be useful in the definition of the critical Reynolds number, $Re_{F,crit}$, at which both damping layers, near the wall and near the water surface, merge, completely removing the turbulent core. The critical Reynolds number, for the case of heating, is determined, from [5]:

$$Re_{FL,crit} = \frac{97}{Ka^{0.1}} \quad (22)$$

The eddy diffusivity in this model is then given by:

$$\varepsilon_M^+ = -0.5 + 0.5 \left[1 + 4K^2 y^{+2} \left(1 - \frac{y^+}{h^+} \right)^2 \times \left\{ 1 - \exp \left[-\frac{y^+}{A^+} \left(1 - \frac{y^+}{h^+} \right) \right]^{1/2} \times \left(1 - \frac{0.865 Re_{FL,crit}^{1/2}}{h^+} \right) \right\}^2 \right]^{1/2} \quad (23)$$

The best way to adapt this model to a shear-driven film is to introduce a dimensionless number similar to that defined by (21), accounting for the influence of shear stress instead of gravity, and then to find, either experimentally or theoretically, the relationship between $Re_{FL,crit}$ and this number (see Appendix A). This, however, would be a laborious procedure, since, to the best of our knowledge, a correlation of this kind has not yet been investigated. Another way of adapting this model to a shear-driven film is to perform calculations using definition (19) together with the definition of the laminar sublayer [16]. The simplest way, however, is just to assume that laminarization in both cases, i.e., in the case of both gravity-driven and shear-driven films, occurs under the same dynamical conditions. Taking into account the fact that the definition of the laminarization parameter is obtained from the Nusselt thickness for a freely-falling laminar film [5], this assumption is reasonable,

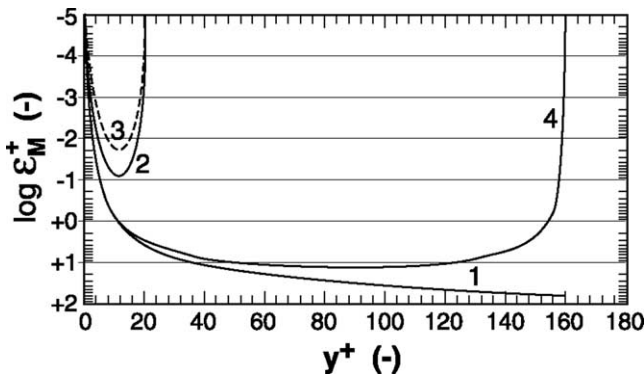


Fig. 2. Eddy diffusivity models for momentum transfer according to various authors: (1) van Driest [8] for the near-the-wall region; (2) Mudawwar and El-Masri [5] for saturated evaporation, $h^+ = 20.5$, $Re_{FL,crit} = \frac{0.04}{Ka^{0.37}}$; (3) [5] for heating, $h^+ = 20.5$, $Re_{FL} = 838$ ($h = 500 \mu\text{m}$, $V_a = 20 \text{ m}\cdot\text{s}^{-1}$); (4) [5] for heating, $h^+ = 160.2$, $Re_{FL} = 1.23 \times 10^4$ ($h = 2 \text{ mm}$; $V_a = 30 \text{ m}\cdot\text{s}^{-1}$).

though not necessarily incontrovertible. In the latter case, the model can be applied directly only by taking into account the temperature dependence of the water properties introduced in the Ka number. Calculations show that, when the temperature of supercooled water varies over the range T_m to T_2 with $\Delta_{bk} = 6 \text{ K}$, the value of Ka varies from 2.4×10^{-10} to 5.18×10^{-10} . Using a value of 3.95×10^{-10} , corresponding to a supercooling of 4 K, one may deduce from (22) that $Re_{FL,crit} = 845.5$. This value will be used in further calculations later in this article.

Fig. 2 presents the profile of eddy diffusivity obtained from the various models, and the results are compared with the near-the-wall behavior of eddy diffusivity obtained from (18). The behavior of the eddy diffusivity for a thin water film near its surface is completely different from its near-the-wall behavior. In Fig. 3, eddy diffusivity profiles obtained from [5] are presented for various dynamical conditions. The regular growth of the average and maximum values of eddy diffusivity, with increasing Reynolds number, can be seen very clearly for the transition region, beyond the transition region, and for the region of developed turbulence. A slight overestimation of the eddy diffusivity is obtained for the region of laminar flow.

Eddy diffusivity may not vanish completely at the air–aerosol/water interface due to:

- (i) the instantaneous rupture of the thin water film at wave crests, with consequent droplet ejection; or
- (ii) very strong influence of the waves; or
- (iii) the powerful bombardment of the air–aerosol/water interface by large droplets.

As a consequence, wall and interfacial shear stresses will not be equal. This complex case, however, will not be discussed in this paper. In summary, one may say that the question of the general shape of the eddy diffusivity function near the wavy, sheared interface still remains unanswered.

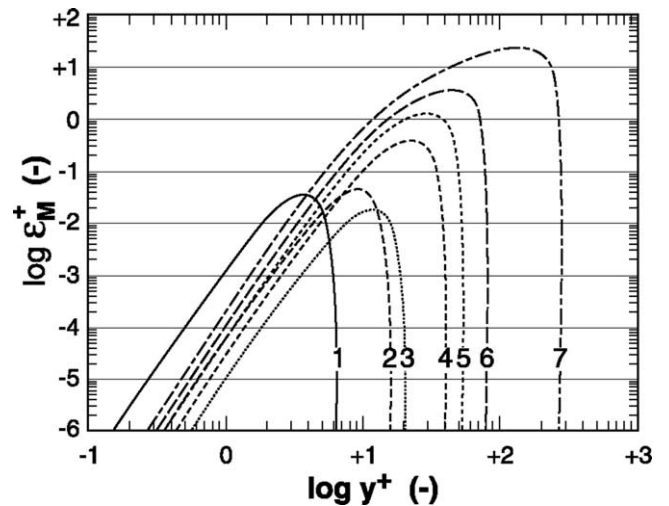


Fig. 3. The behavior of eddy diffusivity [5] in a water film of various thicknesses, as a function of normal distance from the wall, for Reynolds numbers in the transition region with heating: (1) $h^+ = 6.4$, $Re_{FL} = 80.2$ ($h = 500 \mu\text{m}$, $V_a = 10 \text{ m}\cdot\text{s}^{-1}$); (2) $h^+ = 8$, $Re_{FL} = 126$ ($h = 200 \mu\text{m}$, $V_a = 30 \text{ m}\cdot\text{s}^{-1}$); (3) $h^+ = 20.5$, $Re_{FL} = 837$ ($h = 1 \text{ mm}$, $V_a = 10 \text{ m}\cdot\text{s}^{-1}$); (4) $h^+ = 40$, $Re_{FL} = 2.78 \times 10^3$ ($h = 500 \mu\text{m}$, $V_a = 30 \text{ m}\cdot\text{s}^{-1}$); (5) $h^+ = 53.4$, $Re_{FL} = 3.9 \times 10^3$ ($h = 2 \text{ mm}$, $V_a = 10 \text{ m}\cdot\text{s}^{-1}$); (6) $h^+ = 80.1$, $Re_{FL} = 5.98 \times 10^3$ ($h = 1 \text{ mm}$, $V_a = 30 \text{ m}\cdot\text{s}^{-1}$); (7) $h^+ = 266.9$, $Re_{FL} = 2.12 \times 10^4$ ($h = 5 \text{ mm}$, $V_a = 20 \text{ m}\cdot\text{s}^{-1}$).

This appears to be the principal distinction between wavy, thin film flow and classical turbulent Couette flow, where the eddy diffusivity decreases after attaining a maximum, constant value in the bulk flow [17], similar to the water flow near the free surface in a channel [11].

3.3. Turbulent temperature profile in a supercooled water film under a wavy surface

By using the following definitions

$$T^+ = \frac{T - T_1}{T_\tau} \tag{24}$$

$$T_\tau = \frac{\rho_i L_i \frac{dy_1}{dt}}{\rho_w c_w u_\tau} = \frac{\rho_i L_i a (T_m - T_1)^b}{\rho_w c_w u_\tau} \tag{25}$$

Eq. (2) may be transformed into:

$$\frac{d^2 T^+}{dy^{+2}} = - \frac{dT^+}{dy^+} \frac{d\varepsilon_M^+}{dy^+} \frac{1}{(Pr_t/Pr + \varepsilon_M^+)} \tag{26}$$

where T^+ is the dimensionless temperature; and T_τ is the friction temperature (K). Using the same definitions, the boundary condition (7) may be transformed into:

$$\left. \frac{dT^+}{dy^+} \right|_{y^+=0} = - \frac{1}{(1/Pr + \varepsilon_M^+/Pr_t)} \tag{27}$$

Here, for the purposes of the present work, we will consider a “thermally smooth” surface, i.e., the latent heat emerges precisely at the ice/water interface. Then condition (27) may be written as:

$$\left. \frac{dT^+}{dy^+} \right|_{y^+=0} = - Pr \tag{28}$$

Hence, the Prandtl number defines the slope of the non-dimensional temperature near the ice/water interface. The second boundary condition, obtained from (8), is:

$$T^+|_{y^+=0} = 0 \tag{29}$$

3.4. Results of numerical computation

Both equations for velocity (14) and temperature (27) have the same shape. The numerical solutions were obtained by using a fifth- and sixth-order Runge–Kutta–Fehlberg algorithm, with reducing step-size, allowing a control on the accuracy of the solution by comparing the solutions of the fifth- and sixth-order. The desired accuracies for T^+ and its first derivative were different: for T^+ , the accuracy was higher than for its derivative. The algorithm was implemented using a marching procedure from the ice/water interface to the air/water interface. Equality of the wall and interfacial shear stresses defines the slope of the velocity profile near the wall, i.e., the ice/water interface (3). For the dimensionless temperature, the slope at the marching point is given by (28). The second boundary condition for both equations is given by (4) and (29), respectively.

The application of van Driest’s model [8] for eddy diffusivity reveals a universal law-of-the-wall for both equations. Both solutions, shown in Fig. 4, exhibit the following significant layers [18]:

a pure viscous sublayer

$$0 \leq y^+ \leq 5 \quad \text{where } u^+ = y^+ \tag{30}$$

and

$$0 \leq y^+ \leq 2, \quad T^+ = y^+ \tag{30a}$$

a buffer layer

$$5 < y^+ \leq 70 \quad \text{where } u^+ = -3.5 + 5 \ln y^+ \tag{31}$$

an overlap layer

$$y^+ > 70 \quad \text{where } u^+ = \frac{1}{K} \ln y^+ + C^+ \tag{32}$$

and

$$\lim T^+(y^+, Pr) = \frac{Pr_t}{K} \ln y^+ + C_{T^+}^+(Pr) \tag{33}$$

where the constant in the final temperature distribution depends on the Prandtl number only:

$$C_{T^+}^+ = 13.7 Pr^{2/3} - 7.5 \tag{34}$$

The constant C^+ in the velocity distribution, for smooth surfaces, is typically taken to be 5. For rough surfaces, it is a function of the equivalent sand roughness, k_s . A rigorous approach should consider the dependence of C^+ on the growth rate of the ice/water interface. For the present purpose, however, we will define it only for the stable case, when the growth rate of the ice/water interface equals the growth rate of the water/aerosol interface.

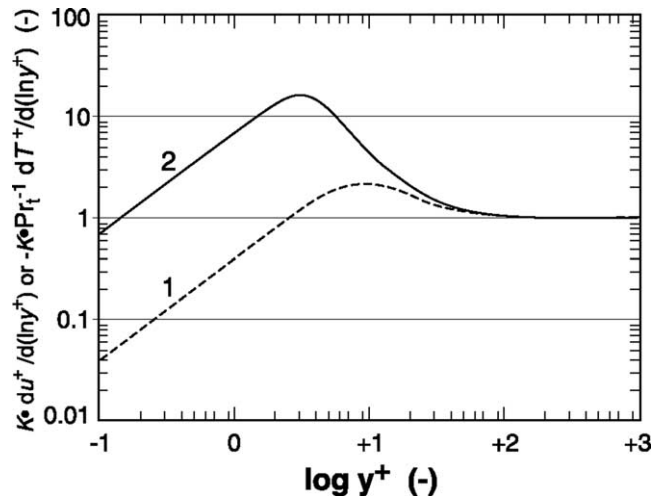


Fig. 4. Universal law-of-the-wall for the fields of: (1) velocity; and (2) temperature.

In order to apply the eddy diffusivity model for thin films [5], we need to specify the dependence of the interfacial shear stress on the water film thickness. Fig. 5 presents the behavior of the air shear stress at the surface of the water film, as employed in further calculations. The values of the air shear stress, calculated according to Eqs. (5) and (6), are compared to the values obtained for air flow over water in a wind-wave tank [6]. The accepted behavior of the air shear stress, with a saturation value attained near the maximum of Re_F , as presented in [3], require some explanation. In [1], we have seen that the formula for the average skin friction coefficient for a rough, flat plate, c_f , describes the experimental data from [3] precisely. This means that a conceptual model that takes into account the features of interfacial waves, especially their amplitude, is correct. Chu and Dukler [19] measured the ratio between substrate wave amplitude and substrate thickness, and compared their data with the results obtained by other authors. This ratio was found to be a saturating function of Re_{FL} , in the range from 10 to 1000, increasing from 0.05 to 0.5. Such a maximum was also predicted by Kapitza (reference in [19]) and Levich [10]. At the same time, it was found that, for constant Re_{FL} , an increase in the gas Reynolds number effects a decrease in film thickness. Accordingly, it is logical to suppose that the shear stress distribution, which is a function of the state of the air–aerosol/water interface, is also a saturating function of water film thickness. Although in their next experimental work, Chu and Dukler [20] obtained a new maximum for this ratio, equal nearly to unity for large waves, with Re_{FL} in the range 500 to 5000, a saturation in the shear stress distribution was found once again. Even more recent investigations [21] recognize four different regimes: smooth; a region of 2-D regular waves; a Kelvin–Helmholtz wave region; and an atomization region, where droplets are sheared off the crests of the waves. The boundaries are mobile, depending on the Re_{FL} and the viscosity of the fluids. Thus, adoption of saturation of the air shear stress

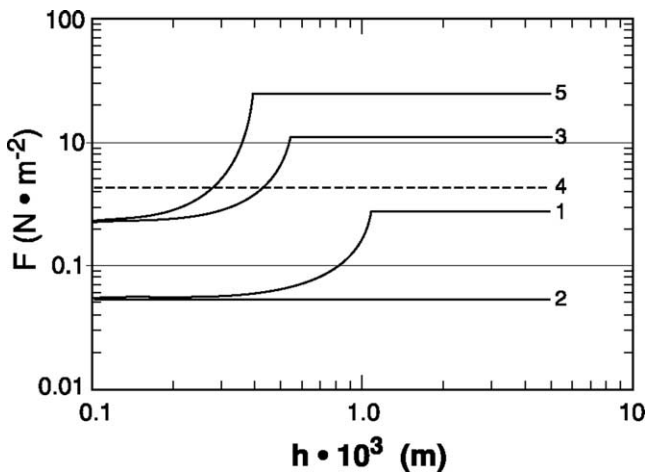


Fig. 5. Typical distributions of interfacial shear stress for concurrent air–water flow as functions of the water film thickness used in the calculations. The case of air flow over a thin water film [3] is compared to the case of air flow over water in a wind-wave tank [6]: (1) thin film, $V_a = 10 \text{ m}\cdot\text{s}^{-1}$; (2) wind-wave tank, $V_a = 10 \text{ m}\cdot\text{s}^{-1}$; (3) thin film, $V_a = 20 \text{ m}\cdot\text{s}^{-1}$; (4) wind-wave tank, $V_a = 20 \text{ m}\cdot\text{s}^{-1}$; (5) thin film, $V_a = 30 \text{ m}\cdot\text{s}^{-1}$.

implies the occurrence of saturation in wave amplitude in the 2-D regular or the Kelvin–Helmholtz wave regimes. Additional increases in the already-saturated value of air shear stress can be related to a change of the mode of interfacial waves, from lower to higher, and a consequent rapid saturation to their new amplitude.

Fig. 6 presents the velocity profiles calculated for various water film Reynolds numbers, in the region of transition and beyond. It makes it possible to compare the resulting profiles with the laminar linear Couette and universal law-of-the-wall turbulent profiles. Below the critical Reynolds number defined by (22), the profile resembles the linear Couette profile. Beyond the critical Reynolds number, the profile deviates considerably from linearity. At the same time, a layer of strong velocity gradient appears near the surface, as a consequence of surface tension damping of the eddy diffusivity. As the Reynolds number increases, the profile resembles the universal law-of-the-wall, with a diminishing damping sublayer near the surface. This sub-layer remains noticeable even for large water film Reynolds numbers ($O \sim 10^4$), though it becomes considerably thinner.

In Fig. 7, the temperature profiles over the water film thickness are presented for the transitional region, as well for the regions before it, and beyond it. In the region before the critical Reynolds number is attained, the profile is appreciably close to linear (curve 1 in Fig. 7). A doubling of the Reynolds number, i.e., for $Re_{FL} = 1.99 \times 10^3$ (curve 2 in Fig. 7), does not change the profile significantly. It is still close to linear, although the deviation from linearity is already noticeable. This trend in the local temperature gradient over the film thickness continues at larger Reynolds numbers, i.e., for $Re_{FL} = 2.53 \times 10^3$ and 3.9×10^3 (curves 3 and 4 in Fig. 7). In the core of the flow, the temperature difference, $T_1 - T_2$, diminishes due to the development of

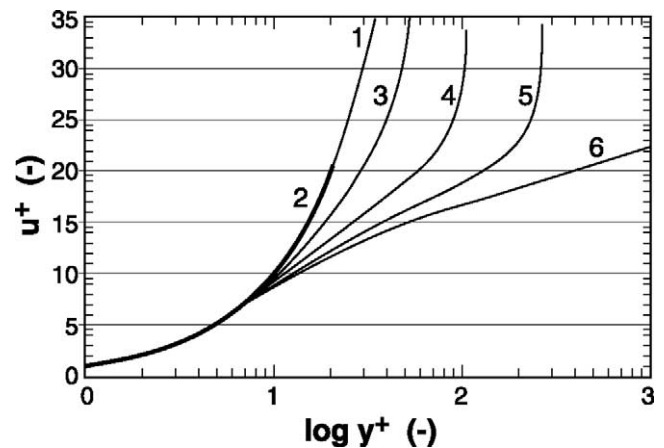


Fig. 6. Calculated velocity profiles for different water film thicknesses compared with the “pure laminar” Couette profile and universal law-of-the-wall turbulent profile: (1) laminar Couette profile $u^+ = y^+$; (2) near-transitional $h^+ = 20.5$, $Re_{FL} = 837.7$ ($h = 500 \mu\text{m}$; $V_a = 20 \text{ m}\cdot\text{s}^{-1}$); (3) post-transitional $h^+ = 53.4$, $Re_{FL} = 3.9 \times 10^3$ ($h = 1 \text{ mm}$; $V_a = 20 \text{ m}\cdot\text{s}^{-1}$); (4) developing turbulent $h^+ = 106.8$, $Re_{FL} = 8.04 \times 10^3$ ($h = 2 \text{ mm}$; $V_a = 20 \text{ m}\cdot\text{s}^{-1}$); (5) developed turbulent for $h^+ = 267$, $Re_{FL} = 2.12 \times 10^4$ ($h = 5 \text{ mm}$; $V_a = 20 \text{ m}\cdot\text{s}^{-1}$); (6) universal law-of-the-wall $u^+ = 1/C^+ + (1/K) \ln y^+$.

new eddy vortices, and the consequent decreasing role of viscous transfer. Near the ice/water and water/air–aerosol interfaces, it increases in order to transfer the energy via an increased temperature gradient. The temperature of the surface of the water film also changes. As well, the temperature difference, $T_1 - T_2$, decreases due mostly to the increase in T_2 . This occurs because the transfer of latent heat from the surface is greater due to larger eddy diffusivity, and hence the rate of displacement of the ice/water interface is faster. Where very large Reynolds numbers of the water film are concerned ($O \sim 10^4$), the subdivision of the water film into sublayers, with completely different characteristic heat transfer mechanisms, has already been completed. There are three sublayers: two very thin viscous sublayers near both interfaces (about 10% in total), where heat transfer occurs exclusively by molecular processes through an increased temperature gradient, and a turbulent core occupying the rest of the film thickness, where the heat transfer occurs exclusively by eddy vortices.

When the near-the-wall eddy diffusivity model [8] is applied, the temperature profiles are completely different from those presented in Fig. 7, as shown in Fig. 8. There is no confinement of turbulence near the water film surface, and the vortex size, i.e., mixing length, continues to grow rapidly, which seems unnatural. In order to preserve the similarity of the dynamical properties, the profiles were calculated for the same Reynolds number. Since the velocity distributions are different, the thickness at which the Reynolds numbers are equalized is also different in both cases. Fig. 9 presents the difference between the thicknesses as a function of Reynolds number. As a consequence of the overestimation of turbulent friction drag near the water surface, with the near-the-wall eddy diffusivity model [8], the calculated thicknesses here

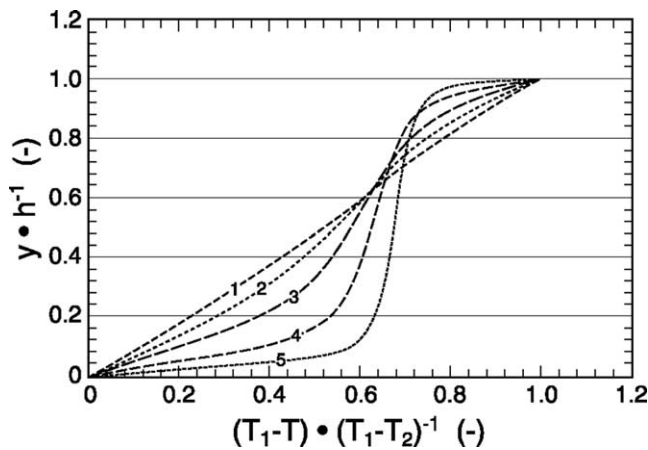


Fig. 7. Temperature profiles in the turbulent supercooled water film calculated with the Mudawwar and El-Masri eddy diffusivity model for heating [5] for various Reynolds numbers: (1) $Re_{FL} = 837.7$ ($h = 500 \mu\text{m}$; $V_a = 20 \text{ m}\cdot\text{s}^{-1}$); (2) $Re_{FL} = 1.99 \times 10^3$ ($h = 600 \mu\text{m}$; $V_a = 20 \text{ m}\cdot\text{s}^{-1}$); (3) $Re_{FL} = 2.53 \times 10^3$ ($h = 700 \mu\text{m}$; $V_a = 20 \text{ m}\cdot\text{s}^{-1}$); (4) $Re_{FL} = 3.9 \times 10^3$ ($h = 1 \text{ mm}$; $V_a = 20 \text{ m}\cdot\text{s}^{-1}$); (5) $Re_{FL} = 8.04 \times 10^3$ ($h = 2 \text{ mm}$; $V_a = 20 \text{ m}\cdot\text{s}^{-1}$).

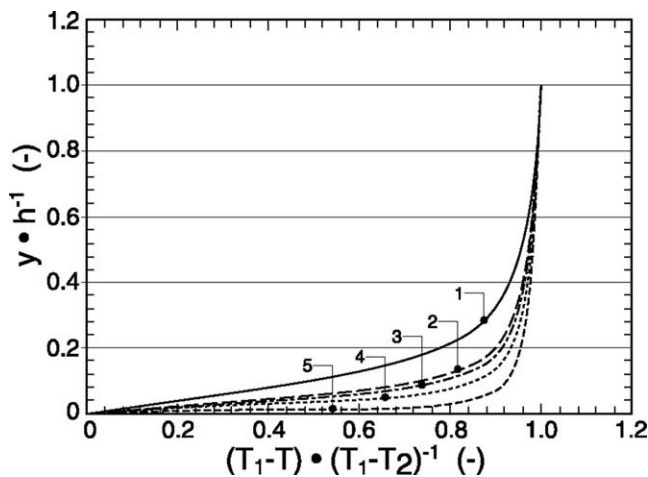


Fig. 8. Temperature profiles in the turbulent water film calculated with the near-the-wall eddy diffusivity model [8] for the same Reynolds numbers as in Fig. 7: (1) $Re_{FL} = 837.7$; (2) $Re_{FL} = 1.99 \times 10^3$; (3) $Re_{FL} = 2.53 \times 10^3$; (4) $Re_{FL} = 3.9 \times 10^3$; (5) $Re_{FL} = 8.04 \times 10^3$.

are greater. The difference is minimal for post-transitional Reynolds numbers, and maximal for developed turbulent flow.

A consideration of the dimensionless solution, T^+ , for the recalculation of the dimensional temperature profile allows us to draw certain conclusions about the regulation of the rate of displacement of the ice/water interface, when there is turbulent heat transfer from this interface. Fig. 10 shows recalculated temperature profiles over the water film thickness. Two very similar thicknesses were employed for the calculation, 1.1 mm and 1.0 mm, with an air velocity of $20 \text{ m}\cdot\text{s}^{-1}$. The calculated Reynolds numbers of 3.9×10^3 and 4.34×10^3 , for both thicknesses, belong to the region of developed turbulence. The temperature profiles were calculated for three values of supercooling at the ice/water inter-

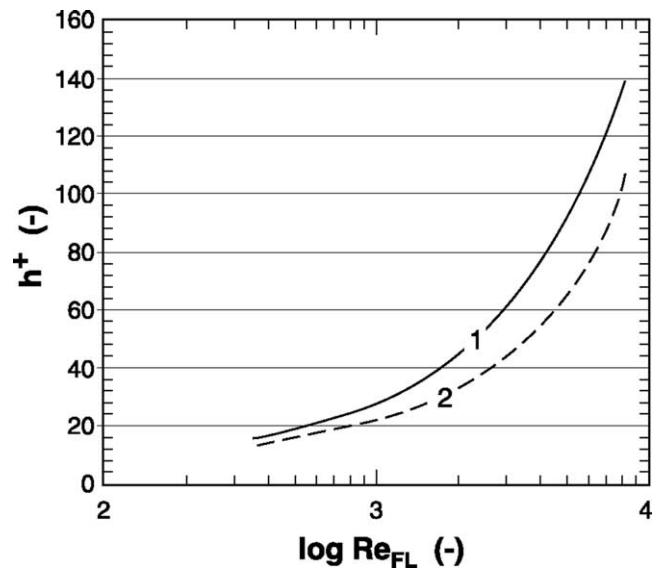


Fig. 9. Conformity between the Reynolds numbers of the dimensionless water film and its thicknesses calculated for different distributions of eddy diffusivities: (1) van Driest [8] near-the-wall model; (2) Mudawwar and El-Masri [5] model for heating.

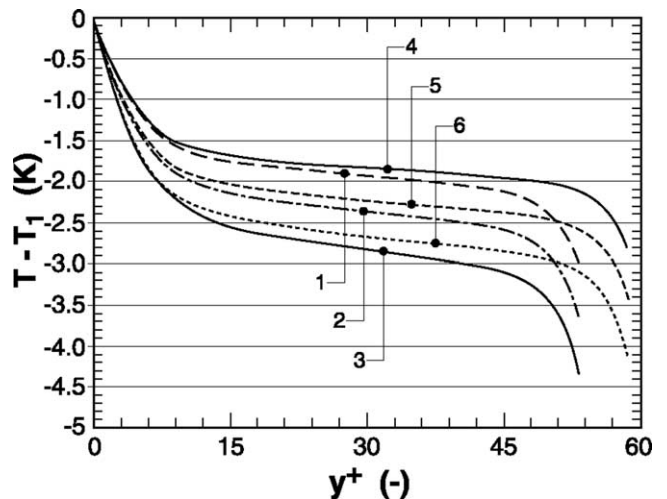


Fig. 10. Temperature distributions in a turbulent supercooled water film for two thicknesses and three supercoolings at the ice/water interface: (1) $h^+ = 53.4$; $\Delta_1 = 0.08 \text{ }^\circ\text{C}$; (2) $h^+ = 53.4$; $\Delta_1 = 0.09 \text{ }^\circ\text{C}$; (3) $h^+ = 53.4$; $\Delta_1 = 0.1 \text{ }^\circ\text{C}$; (4) $h^+ = 58.7$; $\Delta_1 = 0.08 \text{ }^\circ\text{C}$; (5) $h^+ = 58.7$; $\Delta_1 = 0.09 \text{ }^\circ\text{C}$; (6) $h^+ = 58.7$; $\Delta_1 = 0.1 \text{ }^\circ\text{C}$; (1–3) $Re_{FL} = 3.9 \times 10^3$; (4–6) $Re_{FL} = 4.34 \times 10^3$.

face: 0.08 K, 0.09 K and 0.10 K. A difference of only 0.01 K in the supercooling at the ice/water interface corresponds to a difference in air–aerosol/water interface temperature of more than 0.5 K. Such a result emphasizes the importance of the interfacial supercooling for turbulent heat and momentum transfer through the supercooled film. At this point, it is already possible to provide an answer to the question, which was formulated in the accompanying paper [1], attempting to discover the relative significance of supercooling at the ice/water interface and the temperature gradient in its proximity. The appearance of turbulence in the super-

cooled shear-driven water film flowing on an accreting ice surface is a decisive factor which alternates the role of the temperature gradient near the ice/water interface with the role of supercooling at the same interface in the ice accretion process. For a laminar supercooled water film, as shown in [1], the temperature gradient plays the principal role, with the first signs of turbulence, the supercooling at the interface becomes significant. Let us consider one of the three curves for the thicker film. A sudden decrease of film thickness to a lower value corresponds to attaining a point on the curve with the lesser supercooling occurring at the ice/water interface. Conversely, an instantaneous increase of film thickness corresponds to attaining the curve with a greater supercooling at the ice/water interface. In reality, this change will be even more profound than it appears in the figure. These results arise from the fact that changes in the water film thickness produce corresponding changes of the eddy diffusivity defined by (23), and hence the growth rate of the ice/water interface adjusts to changes in the water film thickness. When the water film thickness increases, the growth rate of the ice/water interface accelerates, and vice versa. A similar result for a simplified turbulent case was found by Kachurin [22], who assumed that the eddy diffusivity is proportional to the second power of normal distance from the wall, as proposed by Levich [10]. Furthermore, Kachurin proposed a simplification related to averaging the eddy diffusivity over the water film thickness. In this sense, our more rigorous investigations of laminar and turbulent flow in a freezing water film, have finally proved a thesis, formulated and predicted over 40 years ago, namely that the wet regime of icing is not directly related to the temperature of fusion. Rather, the nature of the icing regime is dictated by the fluid dynamics of the freezing water film on its surface.

3.5. Heat transfer in a turbulent supercooled shear-driven water film

A dimensionless heat transfer coefficient, H^+ , based on the temperature of the water/air-aerosol interface can be defined as follows:

$$H^+ = \frac{Q_{wl} \cdot h}{\lambda_w (T_1 - T_2)} \quad (35)$$

where Q_{wl} is the heat flux evolved at the ice/water interface, which we suppose to be transferred entirely to the surface of the water film, i.e., $Q_{wl} = Q_{out}$.

Using Eqs. (8) and (9), and the formulation for the thickness of a shear-driven water film, (35) may be written:

$$H^+ = \frac{\rho_i L_i a \Delta_1^b}{\rho_w c_w \chi_w (T_m - \Delta_1 - T_2)} \left(\frac{\mu_w Re_{FL} \nu_w}{2F} \right)^{1/2} \quad (36)$$

Using the dimensionless definitions (24) and (25), Eq. (36) can be written:

$$H^+ = - \frac{Pr(T) Re_{FL}^{1/2}}{\sqrt{2} T_2^+ (Ka, Pr, Re_{FL})} \quad (37)$$

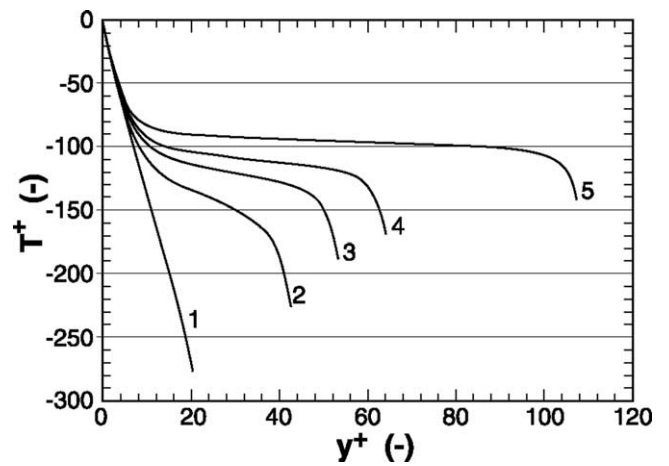


Fig. 11. Dimensionless temperature distribution in a turbulent supercooled water film: (1) $Re_{FL} = 837.7$ ($h = 500 \mu\text{m}$; $V_a = 20 \text{ m}\cdot\text{s}^{-1}$); (2) $Re_{FL} = 3.03 \times 10^3$ ($h = 800 \mu\text{m}$; $V_a = 20 \text{ m}\cdot\text{s}^{-1}$); (3) $Re_{FL} = 3.9 \times 10^3$ ($h = 1 \text{ mm}$; $V_a = 20 \text{ m}\cdot\text{s}^{-1}$); (4) $Re_{FL} = 4.76 \times 10^3$ ($h = 1.2 \text{ mm}$; $V_a = 20 \text{ m}\cdot\text{s}^{-1}$); (5) $Re_{FL} = 8.04 \times 10^3$ ($h = 2 \text{ mm}$; $V_a = 20 \text{ m}\cdot\text{s}^{-1}$).

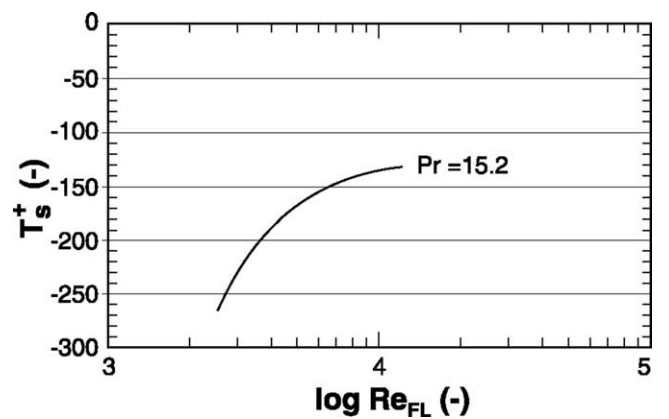


Fig. 12. Typical distribution of dimensionless temperature as a function of the Reynolds number for the water film.

where T_2^+ is the dimensionless temperature of the water surface. The Prandtl number is a function of temperature, and T_2^+ is a function of the Kapitza, Prandtl and Reynolds numbers. If we suppose that the temperature of the water film changes only within a very narrow range of supercooling, then some of these numbers may be taken to be constants, as was assumed when we deduced the critical Reynolds number, where the Kapitza number was taken to be constant. Another form of Eq. (37), taking into account the supercooling at both surfaces, is:

$$H^+ = \frac{T_\tau Pr(T) Re_{FL}^{1/2}}{\sqrt{2} (\Delta_2 - \Delta_1) (Ka, Pr, Re_{FL})} \quad (38)$$

Fig. 11 presents the dimensionless temperature profiles for various film thicknesses, with an air speed of $20 \text{ m}\cdot\text{s}^{-1}$. A typical distribution of the dimensionless temperature of the air-aerosol/water interface is shown in Fig. 12.

4. Conclusions

The thermodynamic and morphological stability of the crystallization front (the interface between the solid and the liquid) under a wind-driven, flowing melt film was investigated here as it relates to disturbances in the external thermodynamic parameters, using the ice–water system as an example. The reaction of the ice crystallization front to disturbances in the thermodynamic parameters was considered for both laminar (see [1]) and turbulent flow with heat transfer through the liquid film. In the laminar regime, where the heat transfer from the crystallization front is conditioned only by the adjoining temperature gradient, the reaction of the interface to disturbances in the thermodynamic parameters is always unstable. This unstable reaction results in corresponding changes in film thickness—either a very fast disappearance of the film, or a rapid thickening of the film until it reaches a stable, turbulent regime.

Completely different behavior is to be found in the case of turbulent flow of a supercooled water film on an icing surface. In this regime, disturbances in the thermodynamic parameters, which lead to changes in film thickness, are eventually damped, restoring the film thickness to its initial value.

We have seen that the ice growth mechanism under a flowing, supercooled water film, accompanied by turbulent heat transfer from the ice/water interface, is self-regulating, and adjusts to random changes over time in the thermodynamic parameters, giving rise to a limiting solution for the case of unstable laminar heat transfer. The presence of convection can stabilize the process, bringing it, for both laminar and turbulent heat transfer events, to a more stable and more rapidly adjusting self-regulating point. For strongly developing convection, especially near the origin of the flow, the two different behaviors can merge into one stable behavior, where the reaction of the ice/water interface is always self-regulating. A distinction between the two regimes of heat transfer from the ice/water interface can be clearly seen in the absence of convection, where the presence of turbulence in the supercooled water film is the crucial factor for the further existence of the film. Otherwise, the film will disappear very quickly, as a consequence of the merging of both interfaces, i.e., the ice/water and air–aerosol/water interfaces. A complete theory explaining how the transition from one mode to another occurs, and using the results obtained in both this paper and the accompanying one [1] will be presented elsewhere [23].

In summary, the following principal conclusions may be drawn from both this and the accompanying [1] papers:

- A physical explanation has been offered for distinguishing the wet and dry regimes of icing. This explanation is related to the dynamics of the water film flowing on the icing surface.
- The presence of turbulence in this supercooled water film is found to be a determining factor for its stability under naturally varying or fluctuating thermodynamic parameters.
- An explicit representation of the flow of supercooled water in icing models will considerably alter the conception of ice accretion modeling.
- Finally, the approach used here for an ice/water transition may have wide applicability to crystallization problems in closely related fields.

Acknowledgements

This study was accomplished within the framework of the NSERC/Hydro-Quebec Industrial Chair on Atmospheric Icing of Power Network Equipment (CIGELE) at the University of Quebec in Chicoutimi, in collaboration with the icing research group at the University of Alberta. The authors would like to acknowledge the associates of the CIGELE and NSERC discovery grant (EPL) for financial support. We also most grateful to M.L. Sinclair for editorial assistance.

Appendix A. Derivation of the modified Kapitza number for the case of a shear-driven water film

The thickness of a freely falling water film flowing under the influence of gravity can be defined by:

$$h^3 = \frac{3\nu_w}{g} \int_0^h u \, dy \quad (\text{A.1})$$

The thickness of a thin film driven by an air shear stress, F , applied at the surface of the film, is defined by:

$$h^2 = \frac{2\mu_w}{F} \int_0^h u \, dy \quad (\text{A.2})$$

By defining the flow integrals through the Reynolds number for the flow as:

$$\int_0^h u \, dy = \frac{\nu_w Re_{FL}}{4} \quad (\text{A.3})$$

and equating the thicknesses in the two cases, one can obtain an expression for the motive power of the flow in the case of a freely falling water film:

$$\rho_w g = \frac{12}{2^{3/2}} \frac{F^{3/2}}{\mu_w^{1/2} \nu_w^{1/2} Re_{FL}^{1/2}} \quad (\text{A.4})$$

The original Kapitza number defined by:

$$Ka = \frac{\mu_w^4 g}{\rho_w \sigma_{w-a}^3} \quad (\text{A.5})$$

may be written in terms of the motive power in gravitational flow as:

$$Ka = \frac{\mu_w^4}{\rho_w^2 \sigma_{w-a}^3} \rho_w g \quad (\text{A.6})$$

By substitution of (A.4) into (A.6), one obtains a modified Kapitza number for the case of a shear-driven film:

$$Ka_{sh} = 6(F\mu_w\nu_w)^{3/2}/\sqrt{2}\sigma_{w-a}^3 Re_{FL}^{1/2} \quad (\text{A.7})$$

This Kapitza number should have a relationship with the critical Reynolds number of the type:

$$Re_{FL,crit} = \alpha Ka_{sh}^\beta \quad (\text{A.8})$$

Since the modified Kapitza number, Ka_{sh} , depends on Re_{FL} , alone, (A.8) may be modified as:

$$Re_{FL,crit}^{1/2+1/\beta} = \alpha N \quad (\text{A.9})$$

where N is another dimensionless number defining the interaction of surface tension and the applied shear stress:

$$N = 6(F\mu_w\nu_w)^{3/2}/\sqrt{2}\sigma_{w-a}^3 \quad (\text{A.10})$$

References

- [1] A.R. Karev, M. Farzaneh, E.P. Lozowski, Character and stability of a wind-driven supercooled water film on an icing surface—I. Laminar heat transfer, *Internat. J. Therm. Sci.*, in press.
- [2] B.L. Messinger, Equilibrium temperature of an unheated icing surface as a function of air speed, *J. Aero. Sci.* 20 (1953) 29–42.
- [3] N.P. Cheremisinoff, E.J. Davis, Stratified turbulent–turbulent gas–liquid flow, *AIChE J.* 25 (1979) 48–56.
- [4] W.B. Hillig, D. Turnbull, Theory of crystal growth in undercooled pure liquids, *J. Chem. Phys.* 24 (1956) 914.
- [5] I.A. Mudawwar, M.A. El-Masri, Momentum and heat transfer across freely-falling turbulent liquid films, *Internat. J. Multiphase Flow* 12 (1986) 771–790.
- [6] S. Komori, R. Nagaosa, Y. Murakami, Turbulence structure and mass transfer across a sheared air–water interface in wind-driven turbulence, *J. Fluid Mech.* 249 (1993) 161–183.
- [7] C. Lorencez, M. Nasr-Esfahany, M. Kawaji, Turbulence structure and prediction of interfacial heat and mass transfer in wavy-stratified flow, *AIChE J.* 43 (1997) 1426–1435.
- [8] E.R. Van Driest, On turbulent flow near a wall, *J. Aero. Sci.* 23 (1956) 1007–1011, 1036.
- [9] S. Komori, H. Ueda, F. Ogino, T. Mizushima, Turbulence structure and transport mechanism at the free surface in an open channel flow, *Internat. J. Heat Mass Transfer* 25 (1982) 513–521.
- [10] V.G. Levich, *Physicochemical Hydrodynamics*, Prentice-Hall, New York, 1962.
- [11] H. Ueda, R. Möller, S. Komori, T. Mizushima, Eddy diffusivity near the free surface of open channel flow, *Internat. J. Heat Mass Transfer* 20 (1977) 1127–1136.
- [12] A. Quarmby, R. Quirk, Measurements of the radial and tangential eddy diffusivities of heat and mass in turbulent flow in a plain tube, *Internat. J. Heat Mass Transfer* 15 (1972) 2309–2327.
- [13] C. Lorencez, M. Nasr-Esfahany, M. Kawaji, M. Ojha, Liquid turbulence structure at a sheared and wavy gas–liquid interface, *Internat. J. Multiphase Flow* 23 (1997) 205–226.
- [14] M. Nasr-Esfahany, M. Kawaji, Turbulence structure under a typical shear induced wave at a liquid/gas interface, *AIChE Symp. Ser., Heat transfer—Houston 92* (1996) 203–210.
- [15] G.L. Hubbard, A.F. Mills, D.K. Chung, Heat transfer across a turbulent falling film with concurrent vapor flow, *J. Heat Transfer Trans. ASME* 98 (1976) 319–320.
- [16] A. Karev, Thermodynamic and radiolocation properties of icing surfaces, Ph.D. Thesis, Russian State Hydrometeorological Institute, Saint Petersburg, Russia, 1993.
- [17] M.M.M. El Telbany, A.J. Reynolds, The empirical description of turbulent channel flows, *Internat. J. Heat Mass Transfer* 25 (1982) 77–86.
- [18] H. Schlichting, K. Gersten, *Boundary Layer Theory*, 8th Revised and enlarged Edition, Springer-Verlag, Berlin, 2000.
- [19] K.J. Chu, A.E. Dukler, Statistical characteristics of thin, wavy films: Part II. Studies of substrate and its wavy structure, *AIChE J.* 20 (1974) 695–706.
- [20] K.J. Chu, A.E. Dukler, Statistical characteristics of thin, wavy films: Part III. Structure of large waves and their resistance to gas flow, *AIChE J.* 21 (1975) 583–593.
- [21] N. Andritsos, Statistical analysis of waves in horizontal stratified gas–liquid flow, *Internat. J. Multiphase Flow* 18 (1992) 465–473.
- [22] L.G. Kachurin, On airplane icing theory, *Izv. Akad. Nauk SSSR, Ser. Geofiz.* 6 (1962) 823–832.
- [23] A.R. Karev, M. Farzaneh, E.P. Lozowski, Character and stability of a wind-driven supercooled water film on an icing surface III. Kineticodynamic theory of solidification in atmospheric icing modeling, in preparation.